

Electronic Supplementary Information

Three-channel fluorescent probe to image mitochondrial stress

Huawei Niu^{a,c}, Jun Tang^a, Xiaofei Zhu^a, Zipeng Li^a, Yongru Zhang^a, Yong Ye^{a,*}, Yufen Zhao^{a,b}

^a *Green Catalysis Center, College of Chemistry, Zhengzhou University, Zhengzhou 450001, P.R. China. E-mail: yeyong03@tsinghua.org.cn*

^b *Institute of Drug Discovery Technology, Ningbo University, Ningbo, 450052, China.*

^c *College of Food and Bioengineering, Henan University of Science and Technology, Luoyang, 471000, China.*

**Corresponding author. * yeyong03@tsinghua.org.cn (Y. Ye). Tel: 139 3907 9373*

Table of contents

Experimental

Fig. S1 Structure characterization of compound **3**

Fig. S2 Structure characterization of probe **NPCIA**

Fig. S3 Normalized fluorescence spectra of donor and absorption spectra of acceptor.

Fig. S4 Absorption and fluorescence emission spectra of **NPCIA** for recognizing HSO_3^- and ClO^-

Fig. S5 A linear relationship between the fluorescence intensity of **NPCIA** and HSO_3^-

Fig. S6 A linear relationship between the fluorescence intensity of **NPCIA** and ClO^-

Fig. S7 Fluorescence spectra of **NPCIA** toward HSO_3^- , ClO^- and other analytes

Fig. S8 Changes in fluorescence of **NPCIA** with HSO_3^- and other analytes ($\lambda_{\text{ex}} = 395$ nm)

Fig. S9 Changes in fluorescence of **NPCIA** with HSO_3^- and other analytes ($\lambda_{\text{ex}} = 544$ nm)

Fig. S10 Changes in fluorescence of **NPCIA** with ClO^- and other analytes

Fig. S11 Time-dependent relationship of the fluorescence changes of **NPCIA** before and after treated with HSO_3^- or ClO^-

Fig. S12 The effect of the pH of the test solution on the pH of **NPCIA** ($\lambda_{\text{em}} = 482$ nm)

Fig. S13 The effect of the pH of the test solution on the pH of **NPCIA** ($\lambda_{\text{em}} = 425$ nm)

Table S1 Determination of HSO_3^- in serum samples

Table S2 Determination of ClO^- in serum samples

Fig. S14 Cytotoxicity were tested in EC1 cells at different **NPCIA** concentrations

Fig. S15 OP and TP imaging of HSO_3^- and ClO^- in EC1 cells, respectively

Fig. S16 Distinguishing between normal cells and cancer cells

Fig. S17 Three-channel imaging of zebrafish with increasing LPS concentration

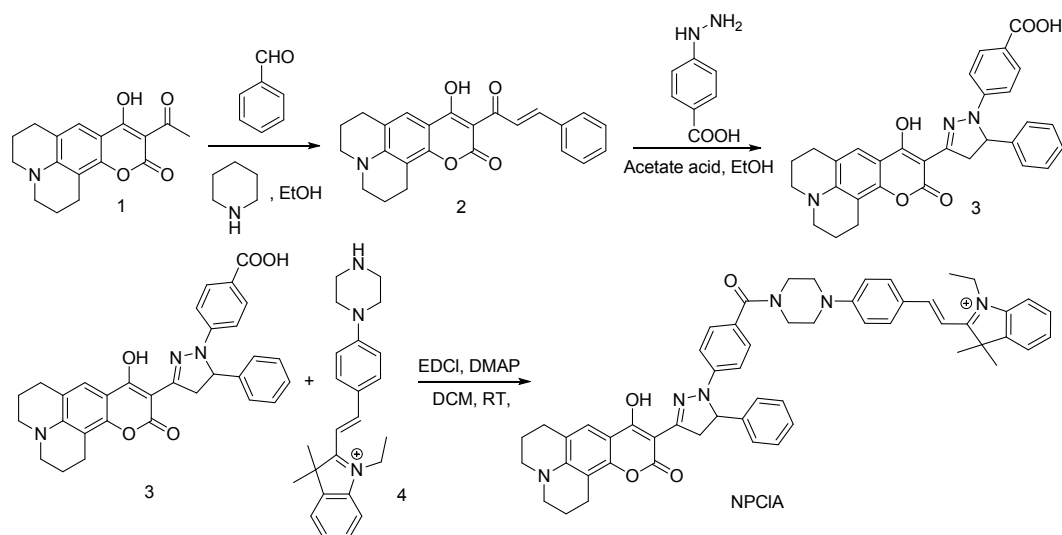
Experimental

Materials and chemicals

3-Aminophenol, malonate, 2,4,6-trichlorophenol, p-hydrazinobenzoic acid, methyl isopropyl ketone and phenylhydrazine were gained from Shanghai Aladdin Biochemical Technology Co., Ltd. N-(3-Dimethylaminopropyl)-N'-ethylcarbodiimide hydrochloride was charged from Shanghai Macklin Biochemical Co., Ltd. 1-bromo-3-chloropropane, pyridine and iodoethane were gained from Shanghai Adamas Reagent Co., Ltd. Mito. Tracker[®] Green FM was gained from Yeasen Biotechnology (Shanghai) Co., Ltd. Fetal Bovine Serum (FBS) was charged from Zhejiang Tianhang Biotechnology Co., Ltd. Newborn Calf Serum (NBCS) and Horse Serum were gained from Zhengzhou Yikang Bio-engineering Co., Ltd.

Instrumentation and equipment

Absorption spectrums were detected by UV-2102 double-beam UV/VIS spectrometer. Fluorescence spectrums were recorded by F-4500 FL Spectrophotometer. The ¹H NMR and ¹³C NMR spectra were measured by Bruker DTX-400 spectrometer. ESI mass spectra were gained by an HPLC Q-Exactive HR-MS spectrometer (Thermo, USA). The pH values were detected by a Model PHS-3C meter (Shanghai, China). Deionized water was used all over the work. Cofocal fluorescence images were gained by Zeiss LSM 880 confocal microscope.



Scheme S1 Synthesis of probe NPCIA.

Synthesis and characterization

Compound 1, 2 and 4 were synthesized according to the reported.^{S1,S2}

Synthesis of compound 3. Compound 2 (194 mg, 0.5 mmol), p-hydrazinobenzoic acid (0.162 g, 1.5 mmol) and acetic acid (0.5 mL) were

added to a 100 mL round bottom flask containing absolute ethanol (25 mL). The reaction mixture was refluxed for 4 h and a yellow solid appeared. After the reaction was completed, it was cooled to room temperature. The precipitate was separated by filtration, washed with frozen ethanol, and dried under vacuum. A yellow solid was obtained as compound **3** (214.4 mg, yield 82.2%). ¹H NMR (400 MHz, DMSO-d₆, ppm): 1.88 (m, 4H), 2.51 (m, 4H), 2.68-2.76 (m, 4H), 3.33 (m, 4H), 4.13 (t, 1H, *J* = 14.4 Hz), 5.49 (s, 1 H), 6.84 (t, 2 H, *J* = 6.4 Hz), 7.34-7.29 (m, 6 H), 7.76 (t, 2 H, *J* = 6.8 Hz), 12.32 (s, 1 H), 13.36 (s, 1 H); ¹³C NMR (100 MHz, DMSO-d₆, ppm): δ = 20.26, 21.20, 27.56, 49.28, 49.84, 61.01, 79.11, 79.44, 79.77, 91.27, 105.28, 111.97, 120.64, 126.13, 128.14, 129.60, 131.50, 160.99, 167.56; HR-MS: *m/z* [M+H]⁺ calculated for [C₃₁H₂₈N₃O₅+H]⁺: 522.2023. Found: 522.2005.

Synthesis of probe NPCIA. Compound **3** (104.2 mg, 0.2 mmol) was added to a solution of anhydrous DCM (10 mL) in an ice bath. EDCl (57.5 mg, 0.3 mmol) and a catalytic amount of DMAP were added, and reacted for 0.5 h. Compound **4** (97.5 mg, 0.2 mmol) dissolved in anhydrous DCM (5 mL) was dropped into the above solution. The ice bath was removed after 0.5 h, and the temperature was gradually raised to room temperature. The reaction was performed at room temperature for 24 h. After the reaction was completed, the reaction mixture was washed with water (10 mL × 3), washed with a saturated sodium chloride solution, dried over anhydrous sodium sulfate, and the separated organic layer was evaporated under reduced pressure. The crude product was purified by column chromatography using DCM/MeOH (20/1, v/v) as mobile phases to obtain the probe NPCIA as a red solid (69.8 mg, yield 35.2%). ¹H NMR (400 MHz, CDCl₃, ppm): 1.60 (t, 3H, *J* = 7.0 Hz), 1.78 (m, 4H), 1.81 (s, 6H), 1.96-2.02 (m, 4H), 2.80-2.88 (m, 4H), 3.28-3.33 (m, 4H), 3.59-3.60 (m, 4H), 3.79 (m, 4H), 4.20-4.28 (m, 1H), 4.85-4.87 (m, 2 H), 5.18-5.23 (m, 1 H), 6.90 (d, 2 H, *J* = 8.6 Hz), 6.99 (d, 2 H, *J* = 8.7 Hz), 7.29-7.38 (m, 8H), 7.41 (s, 1 H), 7.46-7.49 (m, 2H), 7.51-7.59 (m, 3H), 8.10 (d, 1 H, *J* = 15.5 Hz), 8.22 (d, 2 H, *J* = 8.4 Hz); ¹³C NMR (100 MHz, CDCl₃, ppm): δ = 13.94, 20.34, 20.44, 21.41, 27.58, 27.66, 42.87, 46.72, 46.92, 49.64, 50.10, 51.37, 62.44, 91.59, 102.84, 105.73, 106.63, 112.21, 113.38, 114.01, 118.66, 121.13, 122.60, 124.00, 124.52, 125.81, 127.84, 128.38, 129.24, 129.33, 129.43, 135.28, 140.63, 141.53, 142.65, 145.46, 147.37, 150.83, 152.74, 154.75, 154.99, 161.98, 167.46, 170.89, 179.31; HR-MS: *m/z* [M]⁺ calculated for [C₅₅H₅₅N₆O₄]⁺: 863.4279. Found: 863.4271.

Detection Limit Calculation

The detection limit for HSO₃⁻ and ClO⁻ were calculated by the following formula, respectively:

$$\text{Detection limit} = 3 \sigma / |k| \quad (1)$$

Where σ is the standard deviation of the blank measurement and K is the slope of the calibration curve.

The linear relationship between fluorescence intensity and $\text{HSO}_3^-/\text{ClO}^-$ were studied in the range of 1 to 5 equiv. and 0.1 to 0.5 equiv., respectively (for detecting HSO_3^- , $R^2 = 0.99250$; for detecting ClO^- , $R^2 = 0.99395$). Their detection limits were calculated to be 250 nM and 16.6 nM, respectively.

Determination of HSO_3^- and ClO^- in serum samples

Serum samples were diluted 100-fold with the buffer solutions, respectively, and incubated with 10 μM of NPCIA. The reaction progresses were monitored by the fluorescent signal of 482 nm (for detecting HSO_3^-) and 425 nm (for detecting ClO^-), respectively.

Cellular imaging

All cells were cultured in Dulbecco's modified Eagle's medium (DMEM) filled with 10% fetal bovine serum at 37°C.

Cytotoxicity assay. The cytotoxicity assay was performed by using Cell Counting Kit-8 (CCK-8) according to our previously reported method.^{S3} The concentrations of NPCIA were 0, 1 μM , 2 μM , 4 μM , 8 μM , and 16 μM , respectively.

OP and TP imaging. For recognition of HSO_3^- , NPCIA (10 μM) was incubated with EC1 cells for 0.5 h, followed by the addition of HSO_3^- (100 μM) for 0.5 h and imaged; For the identification of ClO^- , NPCIA (10 μM) was incubated with EC1 cells for 0.5 h, followed by the addition of ClO^- (100 μM) and incubated for 0.5 h for imaging. The OP and TP experimental excitation wavelengths of the above probe NPCIA were 405 nm and 780 nm, respectively, and the fluorescence emission wavelengths are 472–502 nm.

Distinguishing between normal cells and cancer cells. NPCIA were incubated with cancer cells (EC1 cells, EC9706 cells, and Hela cells) and normal cells (L929 cells and EC cell s) for 0.5 h, and then imaged under the same conditions. Conditions: For the red channel, $\lambda_{\text{ex}} = 552$ nm, $\lambda_{\text{em}} = 565$ –605 nm; for the green channel, $\lambda_{\text{ex}} = 405$ nm, $\lambda_{\text{em}} = 462$ –502 nm; for the blue channel, $\lambda_{\text{ex}} = 405$ nm, $\lambda_{\text{em}} = 415$ –445 nm.

Mitochondrial colocalization imaging with NPCIA. MCF-7 cells were treated with 10 μM of NPCIA (red channel, $\lambda_{\text{ex}} = 552$ nm, $\lambda_{\text{em}} = 565$ –605 nm) and 1 μM of Mito. Tracker[®] Green FM (green channel, $\lambda_{\text{ex}} = 488$ nm, $\lambda_{\text{em}} = 500$ –550 nm) and co-incubated for 0.5 h. The overlap coefficient for mitochondrial localization experiments was 0.9248.

Three-channel imaging of cell reduction stress effect. NPCIA was incubated with EC1 cells for 0.5 h, followed by the addition of 100 μM and 2 mM of HSO_3^- , respectively, and then incubated for 0.5 h before imaging. Conditions: For the red channel, $\lambda_{\text{ex}} = 552$ nm, $\lambda_{\text{em}} = 565$ –605 nm; for the green channel, $\lambda_{\text{ex}} = 405$ nm, $\lambda_{\text{em}} = 462$ –502 nm; for the blue channel, $\lambda_{\text{ex}} = 405$ nm, $\lambda_{\text{em}} = 415$ –445 nm.

LPS-induced three-channel imaging of oxidative stress. EC1 cells were incubated with 1 μg / mL and 2 μg / mL of LPS for 12 h, followed by adding 10

μM of **NPCIA**, and then incubated for 0.5 h for imaging. Conditions: For the red channel, $\lambda_{\text{ex}} = 552 \text{ nm}$, $\lambda_{\text{em}} = 565\text{-}605 \text{ nm}$; for the green channel, $\lambda_{\text{ex}} = 405 \text{ nm}$, $\lambda_{\text{em}} = 462\text{-}502 \text{ nm}$; for the blue channel, $\lambda_{\text{ex}} = 405 \text{ nm}$, $\lambda_{\text{em}} = 415\text{-}445 \text{ nm}$.

Excess ClO^- -induced three-channel imaging of oxidative stress. HeLa cells were incubated with $10 \mu\text{M}$ of **NPCIA** for 0.5 h, excess ClO^- ($500 \mu\text{M}$) was added, and imaging was performed. Conditions: For the red channel, $\lambda_{\text{ex}} = 552 \text{ nm}$, $\lambda_{\text{em}} = 565\text{-}605 \text{ nm}$; for the green channel, $\lambda_{\text{ex}} = 405 \text{ nm}$, $\lambda_{\text{em}} = 462\text{-}502 \text{ nm}$; for the blue channel, $\lambda_{\text{ex}} = 405 \text{ nm}$, $\lambda_{\text{em}} = 415\text{-}445 \text{ nm}$.

Zebrafish confocal fluorescence imaging

Wild zebrafish were gained from Shanghai Fishbio Co., Ltd. Zebrafish were reared in E3 media at $28 \text{ }^\circ\text{C}$. The 2-day-old zebrafish were incubated with different concentrations of LPS ($0 \mu\text{g/mL}$, $1 \mu\text{g/mL}$ and $3 \mu\text{g/mL}$) for 24 h, respectively, followed by adding $10 \mu\text{M}$ of **NPCIA** and incubating for 1 h, and then imaged by And or Revolution XD spinning disk confocal microscope. Conditions: For red channel, $\lambda_{\text{ex}} = 552 \text{ nm}$, $\lambda_{\text{em}} = 565\text{-}605 \text{ nm}$; for cyan channel, $\lambda_{\text{ex}} = 405 \text{ nm}$, $\lambda_{\text{em}} = 462\text{-}502 \text{ nm}$; for blue channel, $\lambda_{\text{ex}} = 405 \text{ nm}$, $\lambda_{\text{em}} = 415\text{-}445 \text{ nm}$. Scale bar: $200 \mu\text{m}$.

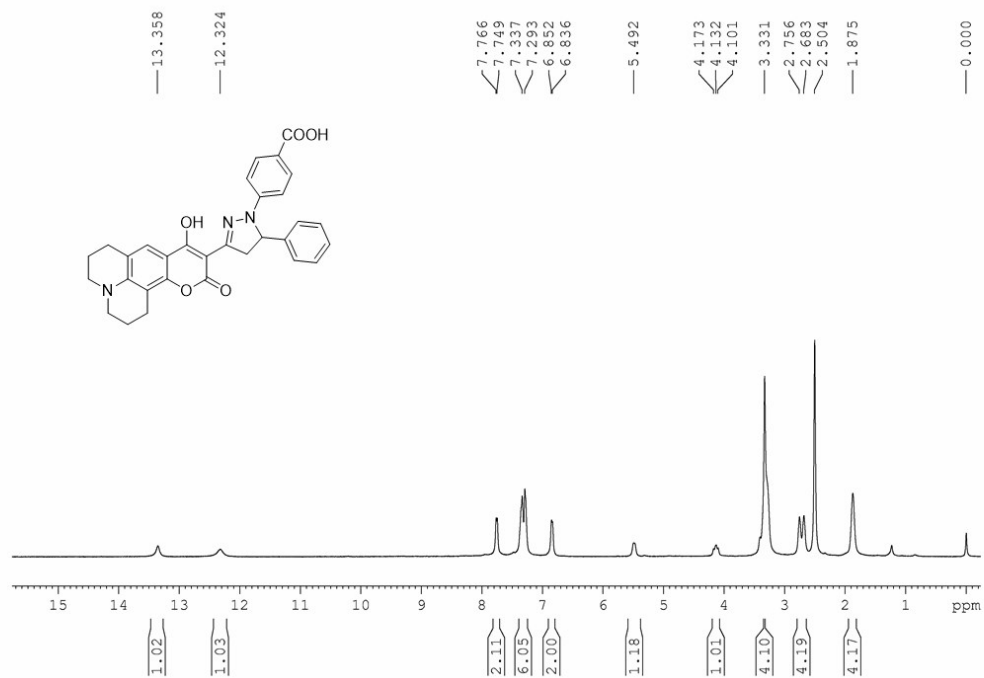
Live subject statement:

Procedures involving animals and their care were conducted in conformity with the guidelines of the Use and Care of Laboratory Animals of National Institutes of Health (NIH Pub. No. 85-23, revised 1996). Ethics committee approval was obtained from the Animal Ethical Experimentation Committee of The First Affiliated Hospital of Zhengzhou University, China.

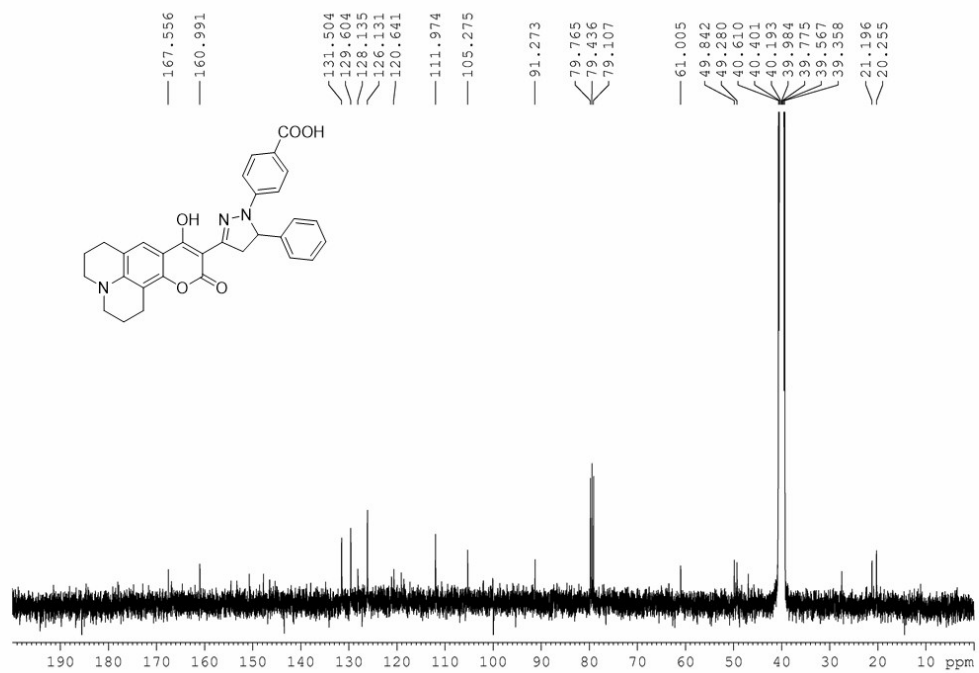
References

- S1 H. Niu, Y. Zhang, F. Zhao, S. Mo, W. Cao, Y. Ye and Y. Zhao, *Chem. Commun.*, 2019, **55**, 9629–9632.
- S2 J. Z. Li, Y. H. Sun, C. Y. Wang, Z. Q. Guo, Y. J. Shen and W. H. Zhu, *Anal. Chem.*, 2019, **91**, 11946–11951.
- S3 X. Yang, W. Liu, J. Tang, P. Li, H. Weng, Y. Ye, M. Xian, B. Tang and Y. Zhao, *Chem. Commun.*, 2018, **54**, 11387–11390.

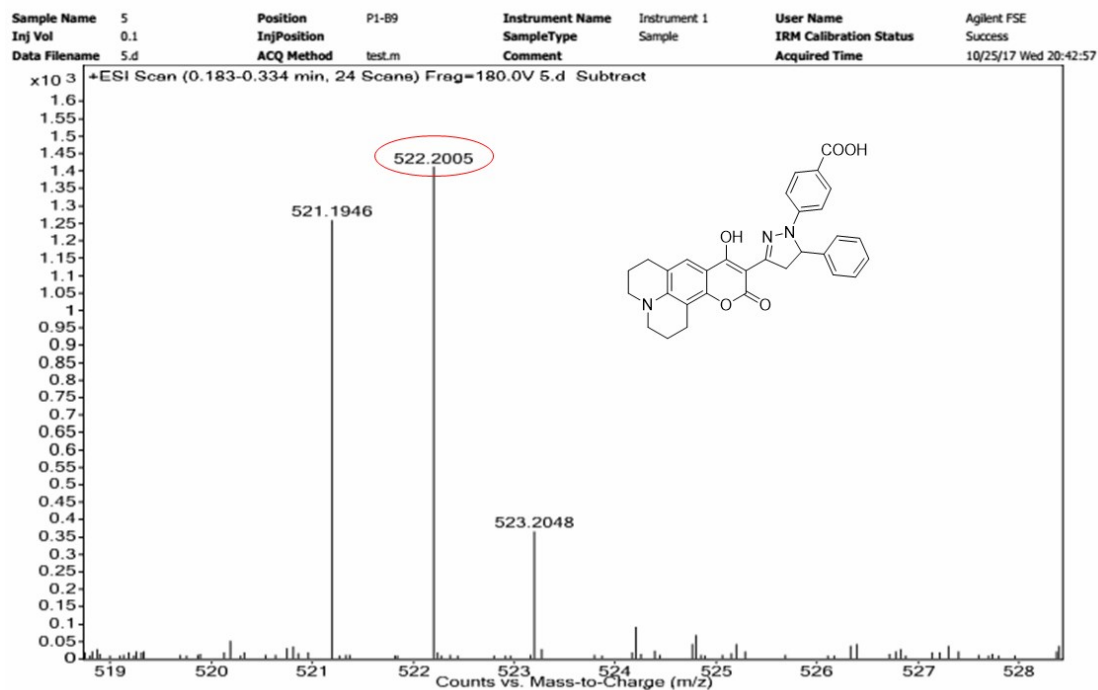
Fig. S1 Structure characterization of compound **3**



¹H-NMR spectrum of compound **3** in DMSO-*d*₆

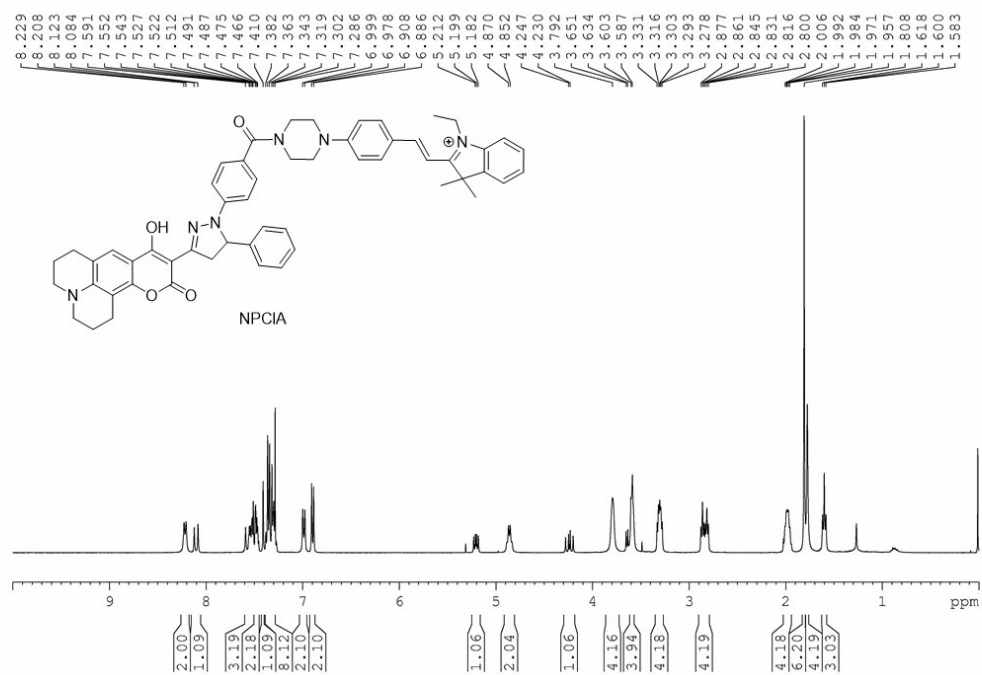


¹³C-NMR spectrum of compound **3** in DMSO-*d*₆

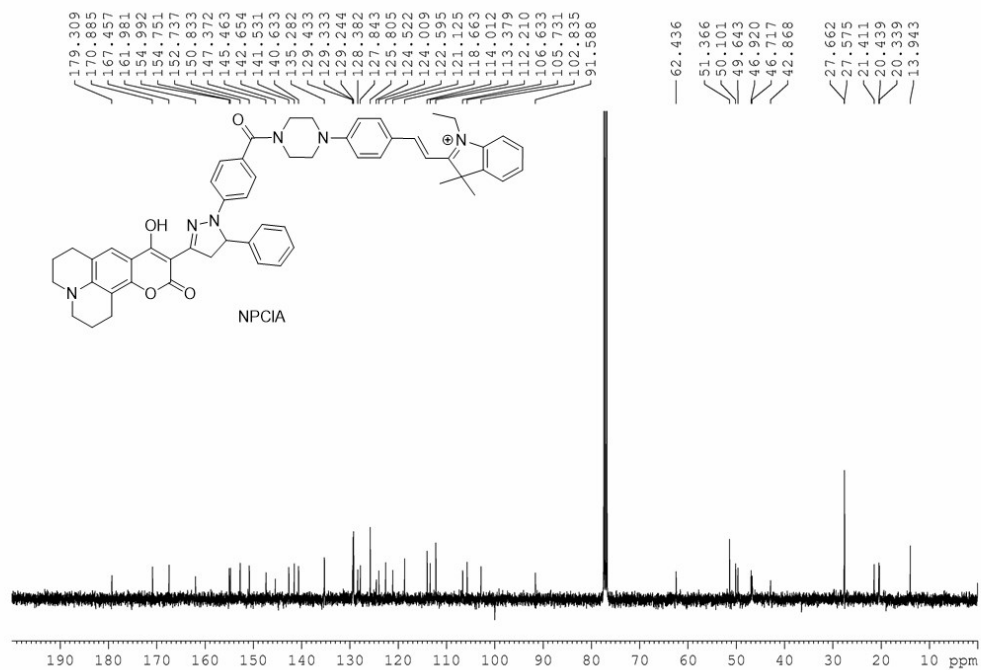


HR-MS spectrum of compound 3

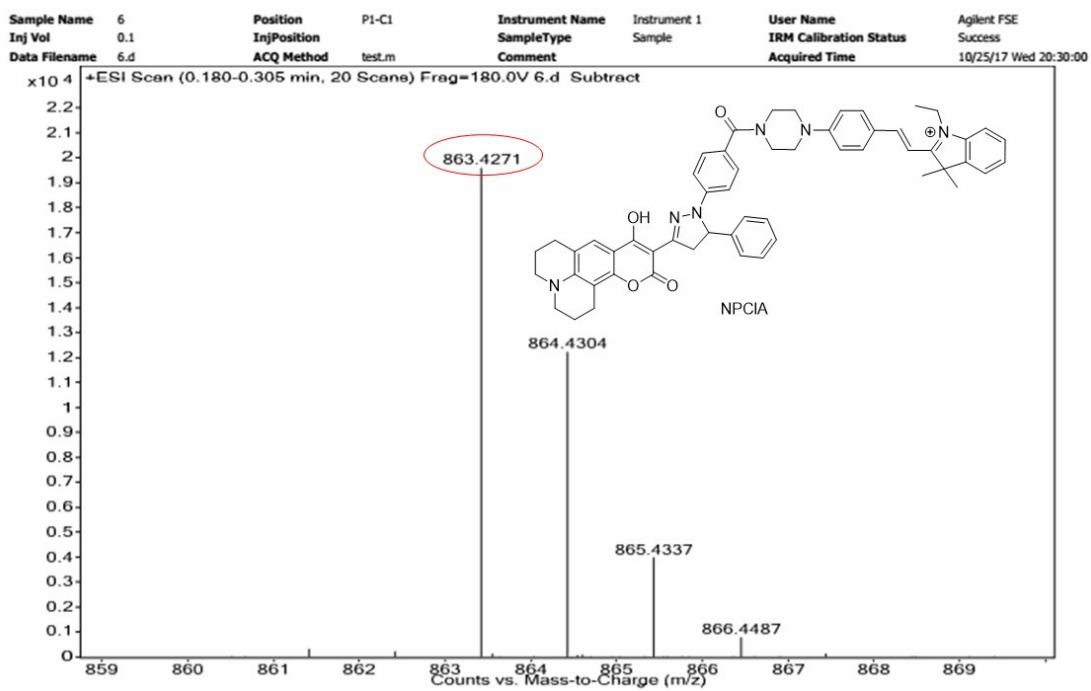
Fig. S2 Structure characterization of probe NPCIA



$^1\text{H-NMR}$ spectrum of probe NPCIA in CDCl_3



^{13}C -NMR spectrum of probe NPCIA in CDCl_3



HR-MS spectrum of probe NPCIA

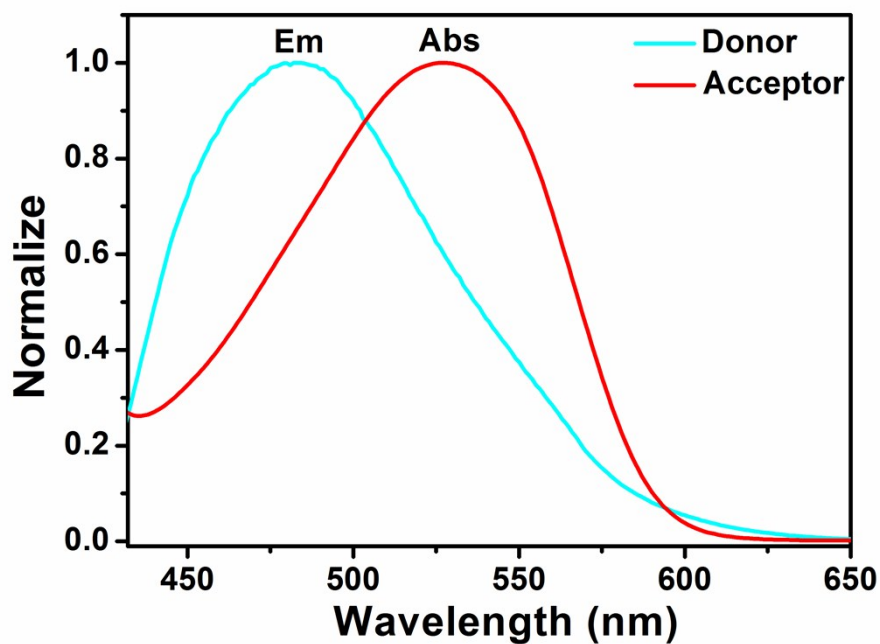


Fig. S3 Normalized fluorescence spectra of donor (coumarin-pyrazoline moiety) and absorption spectra of acceptor (semi-cyanine moiety).

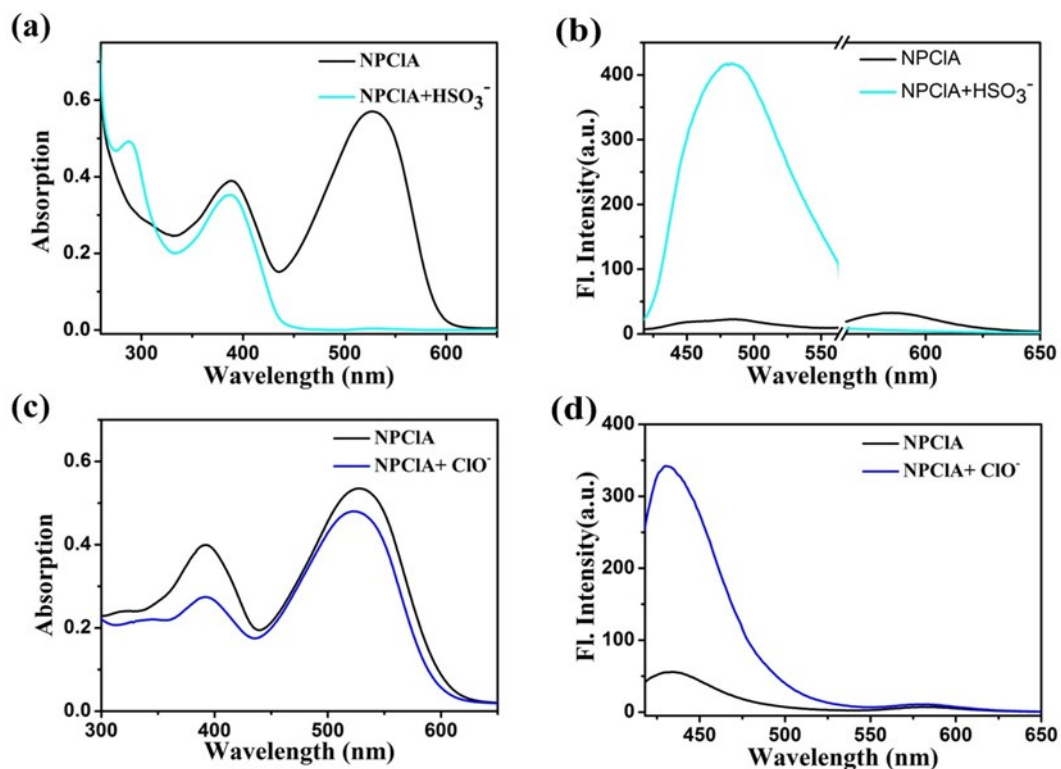


Fig. S4 (a and c) Absorption and (b and d) fluorescence emission spectra of NPCIA for recognizing HSO₃⁻ and ClO⁻. (b) $\lambda_{\text{ex}} = 395$ nm, $\lambda_{\text{em}} = 482$ nm; $\lambda_{\text{ex}} = 544$ nm, $\lambda_{\text{em}} = 585$ nm. (d) $\lambda_{\text{ex}} = 395$ nm, $\lambda_{\text{em}} = 425$ nm. Slit: 10/10 nm.

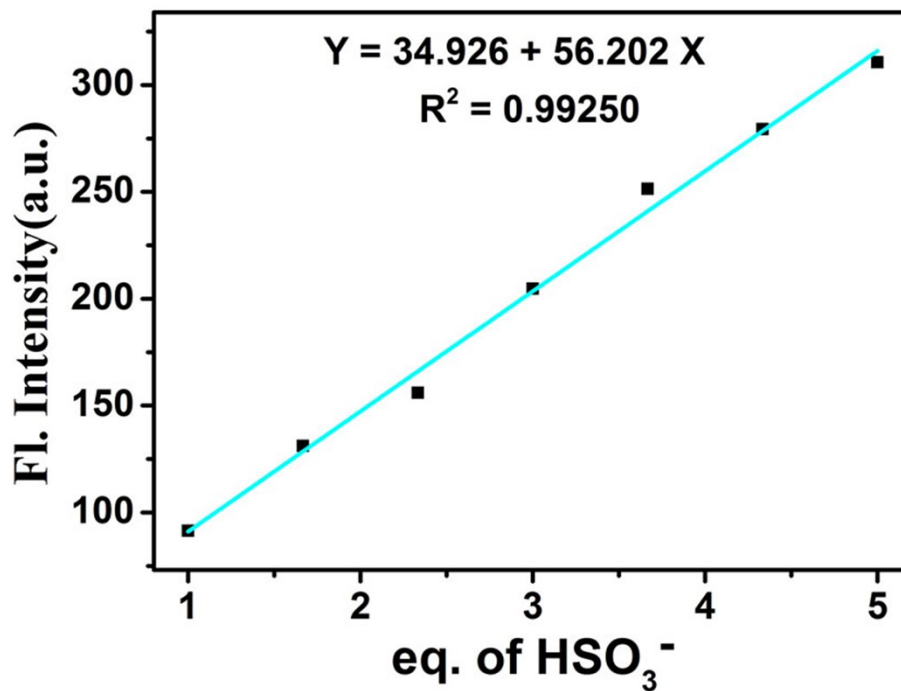


Fig.S5 A linear relationship between the fluorescence intensity of NPCIA and HSO₃⁻ (1-5 equiv.). Conditions: $\lambda_{\text{ex}} = 395 \text{ nm}$, $\lambda_{\text{em}} = 482 \text{ nm}$. Slit: 10/10 nm.

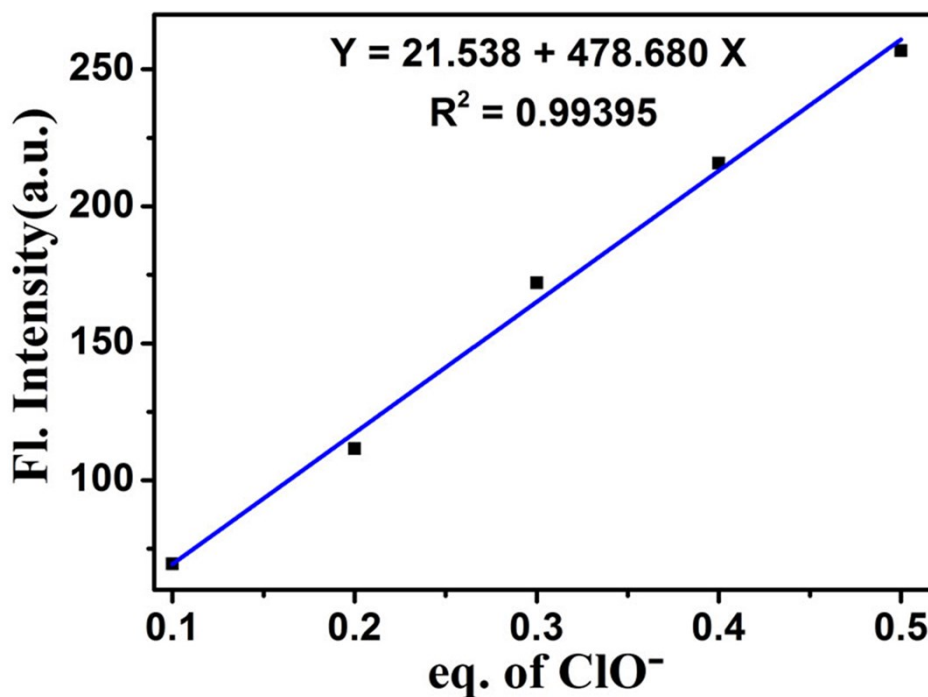


Fig.S6 A linear relationship between the fluorescence intensity of NPCIA and ClO⁻ (0.1-0.5 equiv.). Conditions: $\lambda_{\text{ex}} = 395 \text{ nm}$, $\lambda_{\text{em}} = 425 \text{ nm}$. Slit: 10/10 nm.

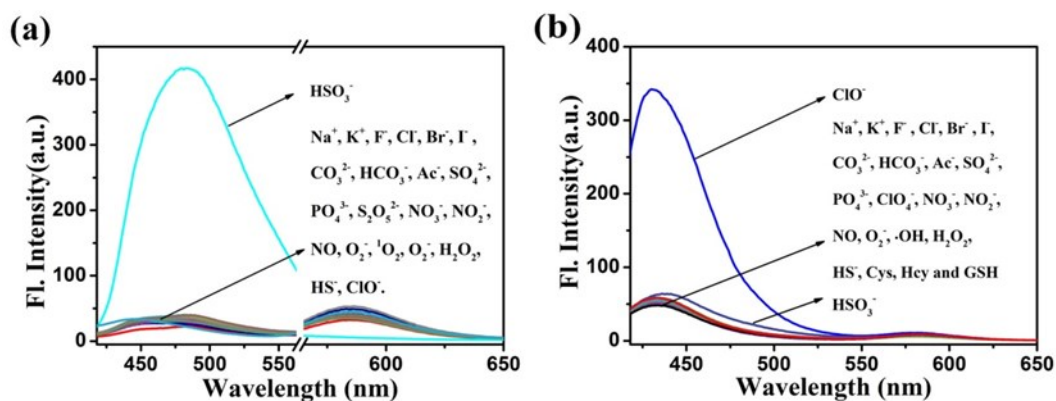


Fig. S7 (a) Changes in fluorescence of NPCIA (10 μM) with HSO₃⁻ (100 μM) and other analytes (100 μM of Na⁺, K⁺, F⁻, Cl⁻, Br⁻, I⁻, CO₃²⁻, HCO₃⁻, Ac⁻, SO₄²⁻, PO₄³⁻, S₂O₅²⁻, HS⁻, NO₃⁻, NO₂⁻, NO•, O₂•⁻, ¹O₂, ClO⁻ and H₂O₂). (b) Changes in fluorescence of NPCIA (10 μM) with ClO⁻ (100 μM) and other analytes (100 μM of Na⁺, K⁺, F⁻, Cl⁻, Br⁻, I⁻, CO₃²⁻, HCO₃⁻, Ac⁻, SO₄²⁻, PO₄³⁻, ClO₄⁻, HS⁻, HSO₃⁻, Cys, Hcy, GSH, NO₃⁻, NO₂⁻, •OH, NO•, O₂•⁻ and H₂O₂). Conditions: (a) λ_{ex} = 395 nm, λ_{em} = 482 nm; λ_{ex} = 544 nm, λ_{em} = 585 nm. (b) λ_{ex} = 395 nm, λ_{em} = 425 nm. Slit: 10/10 nm.

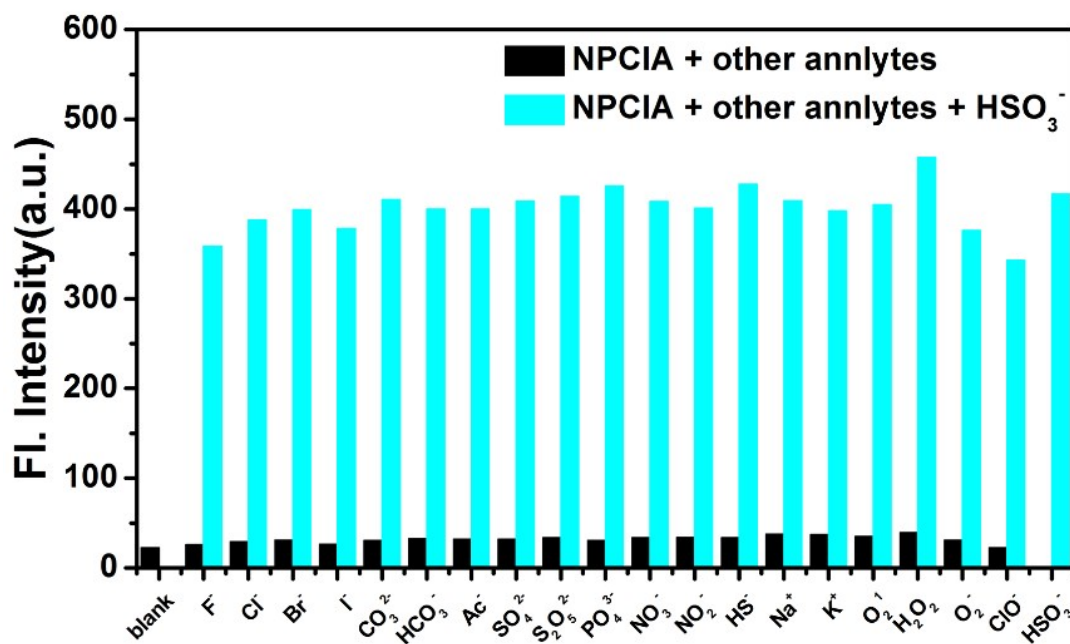


Fig. S8 Changes in fluorescence of NPCIA (10 μM) at 482 nm with HSO₃⁻ (100 μM) and other analytes (100 μM of Na⁺, K⁺, F⁻, Cl⁻, Br⁻, I⁻, CO₃²⁻, HCO₃⁻, Ac⁻, SO₄²⁻, PO₄³⁻, S₂O₅²⁻, HS⁻, NO₃⁻, NO₂⁻, NO•, O₂•⁻, ¹O₂, ClO⁻ and H₂O₂). Conditions: λ_{ex} = 395 nm. Slit: 10/10 nm.

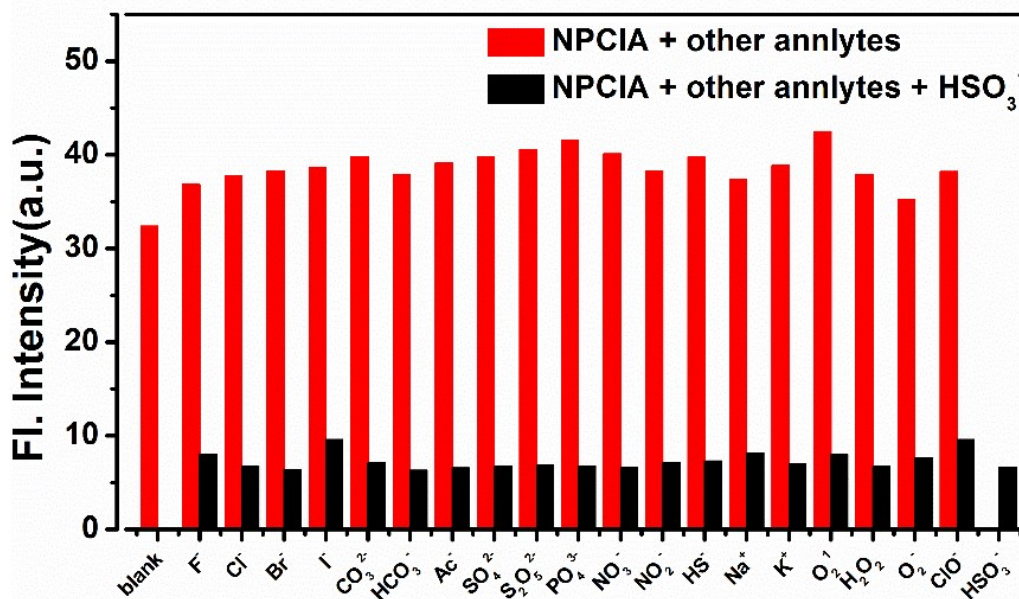


Fig. S9 Changes in fluorescence of NPCIA (10 μM) at 585 nm with HSO_3^- (100 μM) and other analytes (100 μM of Na^+ , K^+ , F^- , Cl^- , Br^- , I^- , CO_3^{2-} , HCO_3^- , Ac^- , SO_4^{2-} , PO_4^{3-} , $\text{S}_2\text{O}_5^{2-}$, HS^- , NO_3^- , NO_2^- , $\text{NO}\cdot$, $\text{O}_2\cdot^-$, $^1\text{O}_2$, ClO^- and H_2O_2). Conditions: $\lambda_{\text{ex}} = 544$ nm. Slit: 10/10 nm.

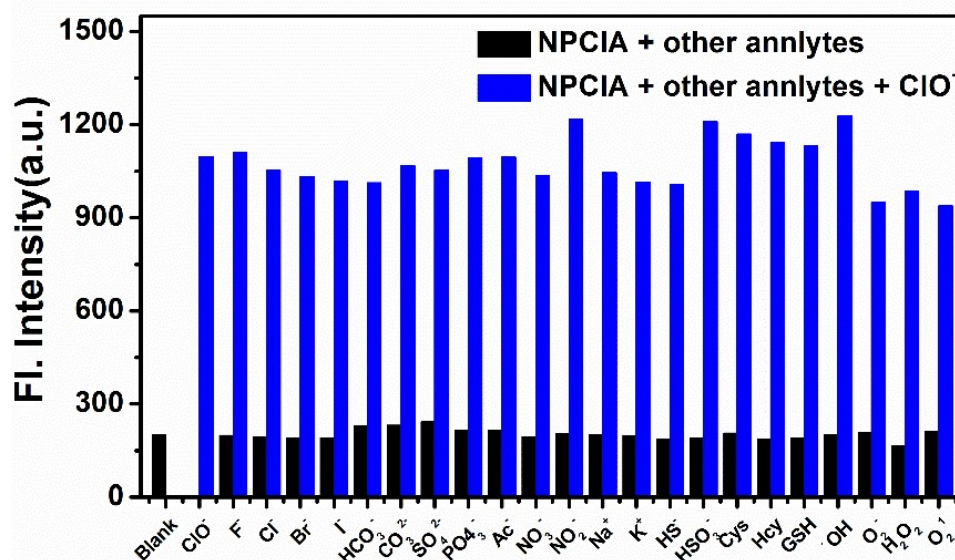


Fig. S10 Changes in fluorescence of NPCIA (10 μM) with ClO^- (100 μM) and other analytes (100 μM of Na^+ , K^+ , F^- , Cl^- , Br^- , I^- , CO_3^{2-} , HCO_3^- , Ac^- , SO_4^{2-} , PO_4^{3-} , ClO_4^- , HS^- , HSO_3^- , Cys, Hcy, GSH, NO_3^- , NO_2^- , $\cdot\text{OH}$, $\text{NO}\cdot$, $\text{O}_2\cdot^-$ and H_2O_2). Conditions: $\lambda_{\text{ex}} = 395$ nm, $\lambda_{\text{em}} = 425$ nm. Slit: 10/10 nm.

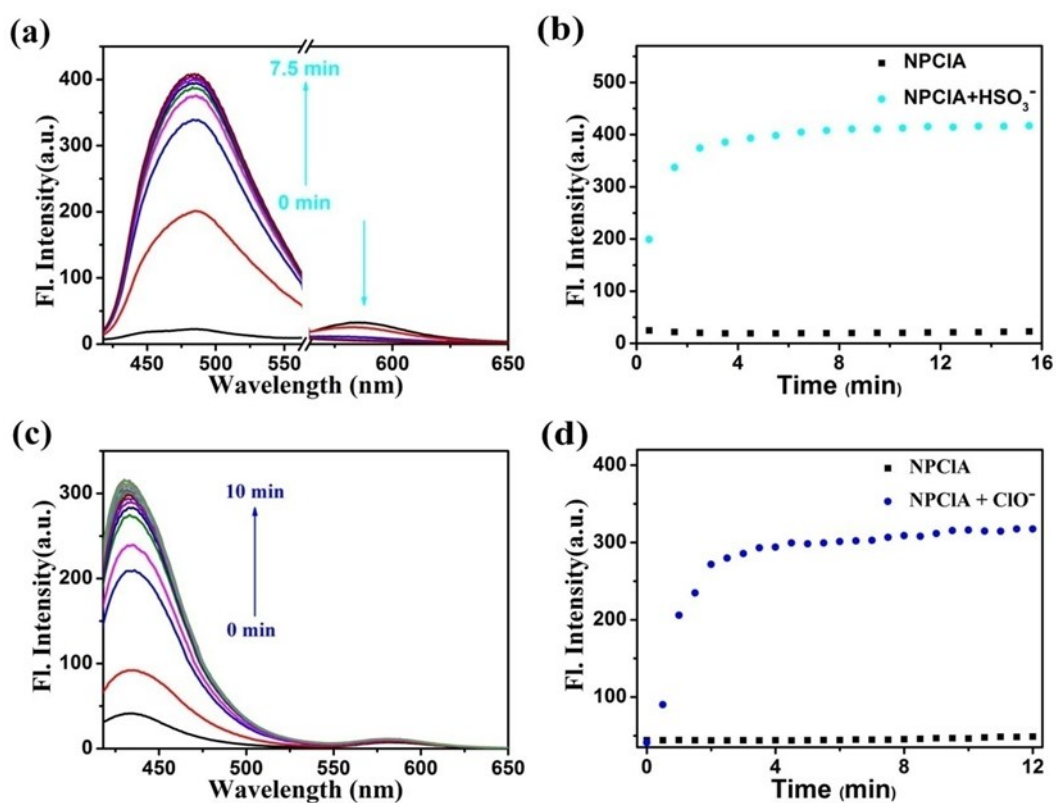


Fig. S11 Time-dependent relationship of the fluorescence changes of NPCIA (10 μM) before and after treated with 10 equiv. of HSO₃⁻ or ClO⁻. Conditions: (a-b) $\lambda_{\text{ex}} = 395$ nm, $\lambda_{\text{em}} = 482$ nm; $\lambda_{\text{ex}} = 544$ nm, $\lambda_{\text{em}} = 585$ nm. (c-d) $\lambda_{\text{ex}} = 395$ nm, $\lambda_{\text{em}} = 425$ nm. Slit: 10/10 nm.

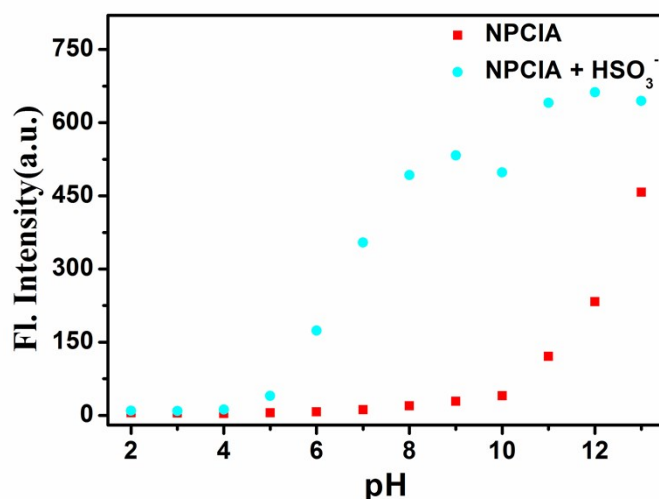


Fig. S12 The pH effect of the test solution on NPCIA (10 μM) was tested in the absence or presence of HSO₃⁻ (10 equiv.). Conditions: $\lambda_{\text{ex}} = 395$ nm, $\lambda_{\text{em}} = 482$ nm. Slit: 10/10 nm.

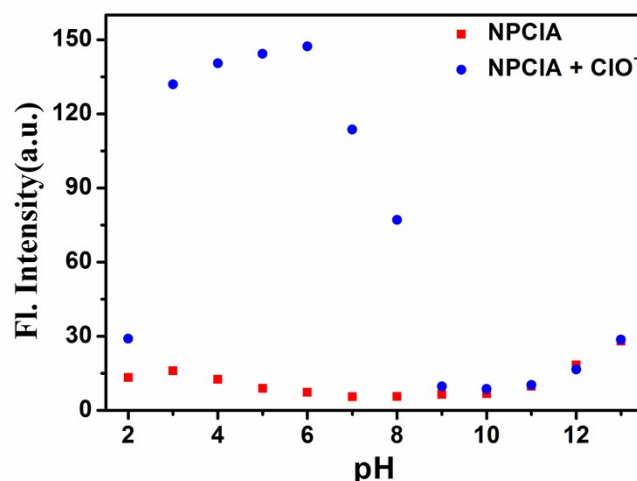


Fig. S13 The pH effect of the test solution on NPCIA (10 μM) was tested in the absence or presence of ClO^- (10 equiv.). Conditions: $\lambda_{\text{ex}} = 395 \text{ nm}$, $\lambda_{\text{em}} = 425 \text{ nm}$. Slit: 10/10 nm.

Table S1 Determination of HSO_3^- in serum samples

Sample	Spiked (μM)	Found (μM)	Recovery (%)	RSD (n = 3, %)
Fetal Bovine Serum (FBS)	0	1.33	-	2.01
	5	6.87	108.57	0.33
	10	13.32	117.56	0.05
Newborn Calf Serum (NBCS)	0	1.40	-	1.87
	5	7.24	113.22	3.09
	10	23.89	113.10	2.05
Horse Serum	0	1.36	-	0.20
	5	6.10	95.79	2.51
	10	12.27	107.99	3.50

Table S2 Determination of ClO^- in serum samples

Sample	Spiked (μM)	Found (μM)	Recovery (%)	RSD (n = 3, %)
Fetal Bovine Serum (FBS)	0	0.41	-	1.03
	1	1.42	99.28	1.69
	3	3.78	110.94	3.04
Newborn Calf	0	0.52	-	3.48

Serum (NBCS)				
	1	1.41	93.00	0.72
	3	3.71	105.51	1.78
Horse Serum				
	0	0.45	-	1.00
	1	1.34	92.99	2.23
	3	3.17	91.93	1.99

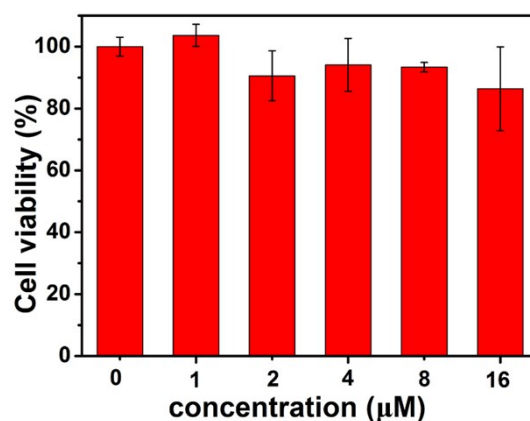


Fig. S14 Cytotoxicity were tested in EC1 cells at different NPCIA concentrations (0, 1 μM , 2 μM , 4 μM , 8 μM , and 16 μM).

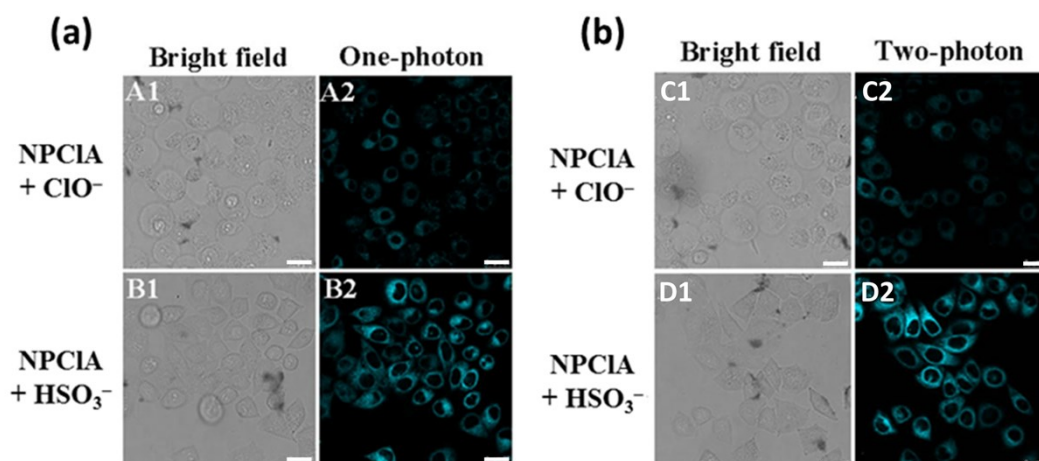


Fig. S15 OP and TP imaging of HSO_3^- and ClO^- in EC1 cells, respectively. NPCIA (10 μM) was incubated with EC1 cells for 0.5 h, followed by adding (A and C) 100 μM of HSO_3^- and (B and D) 100 μM of ClO^- were added to incubate for 0.5 h, respectively, and then imaged. Conditions: for OP imaging, $\lambda_{\text{ex}} = 405 \text{ nm}$; for TP imaging, $\lambda_{\text{ex}} = 780 \text{ nm}$. $\lambda_{\text{em}} = 472\text{--}502 \text{ nm}$. Scale bar: 25 μm .

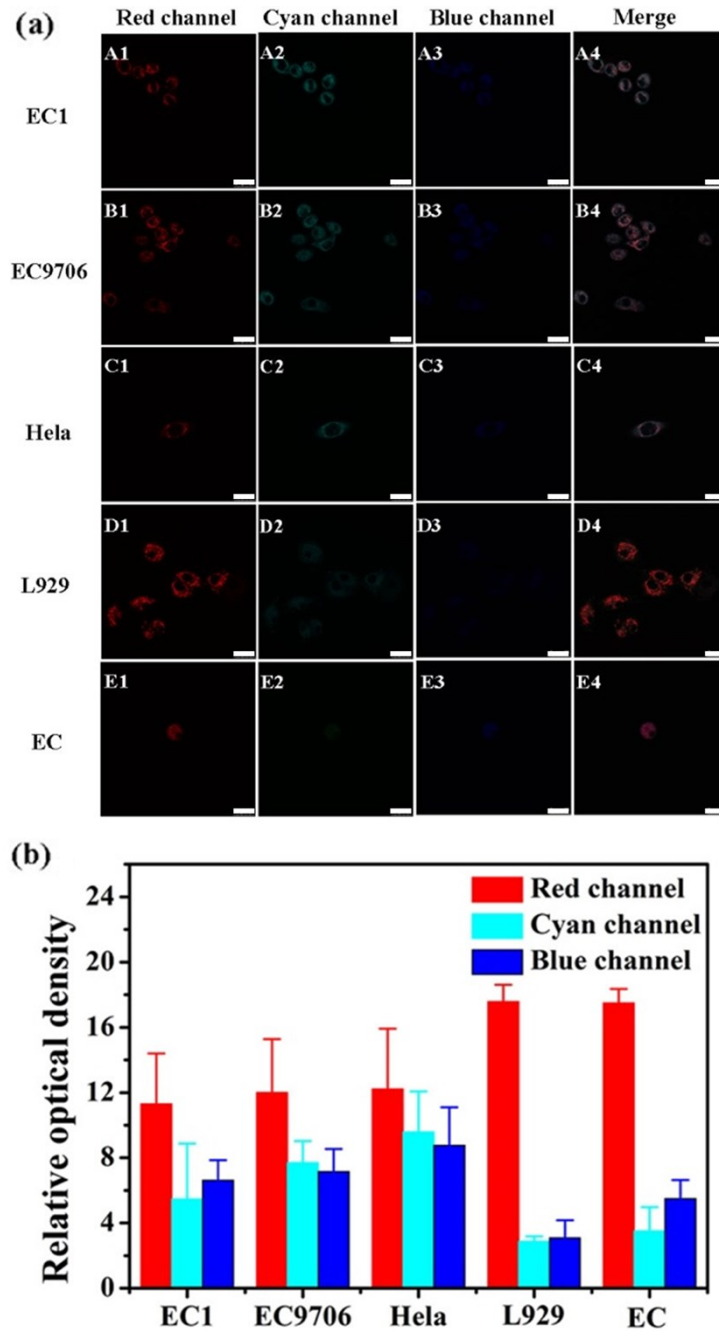


Fig. S16 Three-channel imaging of cancer cells and normal cells. NPCIA was incubated with cancer cells (EC1 cells, EC9706, and Hela cells) and normal cells (L929 cells and EC) for 0.5 h. Conditions: For the red channel, $\lambda_{\text{ex}} = 552 \text{ nm}$, $\lambda_{\text{em}} = 565\text{-}605 \text{ nm}$; for the cyan channel, $\lambda_{\text{ex}} = 405 \text{ nm}$, $\lambda_{\text{em}} = 462\text{-}502 \text{ nm}$; for the blue channel, $\lambda_{\text{ex}} = 405 \text{ nm}$, $\lambda_{\text{em}} = 415\text{-}445 \text{ nm}$. Scale bar: $25 \mu\text{m}$.

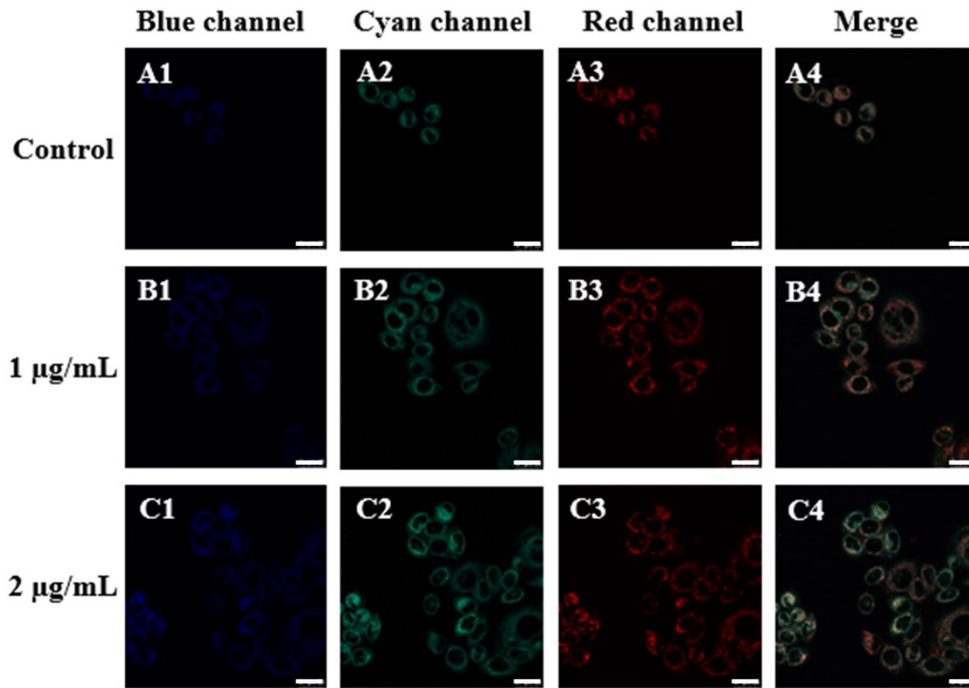


Fig.S17 Three-channel imaging of EC1 cells with increasing LPS concentration. EC1 cells were incubated with different concentrations of LPS (1 $\mu\text{g/mL}$ and 2 $\mu\text{g/mL}$) for 12 h, respectively, followed by adding 10 μM of NPC1A, and then incubated for 0.5 h before imaging. (A4-C4) Merged images of blue channel, cyan channel and red channel. Conditions: For red channel, $\lambda_{\text{ex}} = 552 \text{ nm}$, $\lambda_{\text{em}} = 565\text{--}605 \text{ nm}$; for cyan channel, $\lambda_{\text{ex}} = 405 \text{ nm}$, $\lambda_{\text{em}} = 462\text{--}502 \text{ nm}$; for blue channel, $\lambda_{\text{ex}} = 405 \text{ nm}$, $\lambda_{\text{em}} = 415\text{--}445 \text{ nm}$. Scale bar: 25 μm .

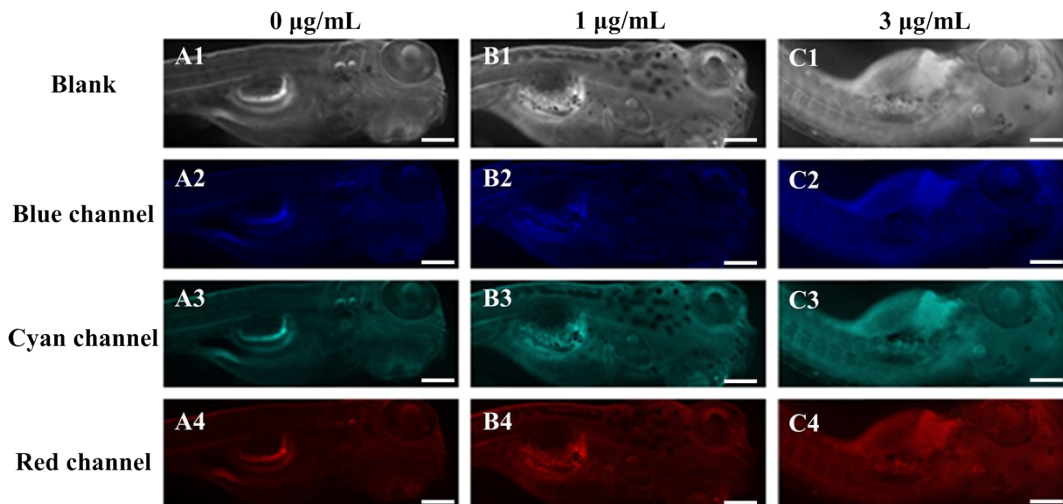


Fig. S18 Three-channel imaging of zebrafish with increasing LPS concentration. Zebrafish were incubated with different concentrations of LPS (0 $\mu\text{g/mL}$, 1 $\mu\text{g/mL}$ and 3 $\mu\text{g/mL}$) for 24 h, respectively, followed by adding 10 μM of NPC1A, and then incubated for 1 h before imaging. Conditions: For red channel, $\lambda_{\text{ex}} = 552 \text{ nm}$, $\lambda_{\text{em}} = 565\text{--}605 \text{ nm}$; for cyan channel, $\lambda_{\text{ex}} = 405 \text{ nm}$, $\lambda_{\text{em}} = 462\text{--}502 \text{ nm}$; for blue channel, $\lambda_{\text{ex}} = 405 \text{ nm}$, $\lambda_{\text{em}} = 415\text{--}445 \text{ nm}$. Scale bar: 200 μm .